

## MUTUAL COMPENSATION OF WAKEFIELD AND CHROMATIC EFFECTS OF INTENSE LINAC BUNCHES\*

J. T. Seeman and N. Merminga

*Stanford Linear Accelerator Center,  
Stanford University, Stanford, CA 94309*

### ABSTRACT

Mutual compensation of transverse and chromatic effects for intense electron bunches in a high-energy linac is a recent Novosibirsk idea which provides a new control of emittance enlargement. In this paper we elaborate on the principles and constraints for this new technique which requires careful matching of internal bunch parameters with external forces. With specific values of the bunch length, bunch intensity, and klystron phasing, the transverse-wakefield-induced forces within the bunch can be cancelled by energy-dependent forces from the quadrupole lattice at all positions along the linac. Under these conditions the tolerances for quadrupole alignment, dipole stability, and injection launch errors are significantly relaxed.

*Contributed to the 1990 Linac Conference  
Albuquerque, New Mexico, September 10-14, 1990*

\* Work supported by Department of Energy contract DE-AC03-76SF00515.

## 1. INTRODUCTION

The primary goal of linear colliders is to maximize the integrated luminosity for the experimental program. Small transverse emittances are a necessary condition for maximum luminosity. However, a number of single-particle and current-dependent effects cause emittance enlargement.<sup>1</sup> In particular, the spectrum of particle energies within the bunch allow chromatic phase-space mixing. Furthermore, current-dependent wakefield effects can result in emittance dilution. A technique<sup>2,3</sup> emanating from the Institute of Nuclear Physics in Novosibirsk called "auto-phasing" can be used to mutually cancel these chromatic and wakefield effects. A description of the physics principles of this technique, the method of application, and an example for the SLC will be discussed in this note.

In Section 2 the difference between auto-phasing and present practice is discussed. In Section 3 we start from the equation of motion of a particle in the presence of transverse wakefields and derive the condition for auto-phasing. Further, we attempt an intuitive discussion of auto-phasing and point out its differences from a method called BNS damping<sup>2</sup> as it has been applied to the Stanford Linear Collider (SLC) linac so far. In Section 4 we describe the procedure used to arrange the linear focusing of a lattice in order for auto-phasing conditions to hold. Finally, in Section 5 we apply the results of this analysis to the SLC linac. Several scenarios are presented.

## 2. PRESENT SITUATION

Off-axis particles traversing an accelerating structure generate transverse wakefields which deflect all trailing particles. There are many causes for a bunch to be off-axis—betatron oscillations, local bumps, head-tail transverse offsets, or collimator deflections. These wakefield deflections accumulate along the linac and cause emittance enlargement of the beam. This beam blowup by wakefields can be reduced by BNS damping. The effect of BNS damping is to reduce the effective defocusing nature of the wakefield force by providing extra focusing for the core and tail particles. This is accomplished by lowering the energy of the trailing particles relative to the head so that the quadrupole lattice focuses them more strongly. The trailing particles are differentially lowered in energy by back-phasing klystrons early in the accelerator and forward-phasing downstream klystrons to keep the energy spectrum small at the maximum energy. The overall goal is to minimize the emittance at the end of the linac using as little extra acceleration as possible. The best configuration depends on many machine parameters and must be calculated for each case. However, with this adaptation of BNS damping the effective emittance is not controlled in the middle of the linac, and sensitivity to local errors is a result.

In this paper we present a new method of controlling transverse wakefields originally suggested by Balakin et al. at the Institute of Nuclear Physics in Novosibirsk.<sup>2,3</sup> This method is based on the phenomenon of auto-phasing: all particles within the bunch—taking into account all forces acting on them—should oscillate with the same amplitude, phase and frequency. The significance of auto-phasing is that the bunch

will remain coherent in its motion independently of any dipole-like perturbations to its trajectory at all locations, and hence the emittance will remain unchanged.

### 3. AUTO-PHASING

Let us assume a relativistic bunch whose transverse dimensions are zero. Let  $x(z, s)$  denote the displacement of a particle in the bunch as a function of  $z$ , the longitudinal position relative to the center of the bunch ( $z$  is positive towards the head of the bunch), and  $s$ , the distance along the accelerator. The approximation of zero transverse dimensions for the bunch is a good one since the transverse dimension of the bunch is very much less than the size of the vacuum chamber.

The equation of motion for  $x(z, s)$  can be written<sup>4</sup>

$$\frac{d}{ds} \left( \gamma(z, s) \frac{d}{ds} x(z, s) \right) + \left( \frac{2\pi}{\lambda(z, s)} \right)^2 \gamma(z, s) x(z, s) = r_0 \int_z^\infty dz' \rho(z') W_\perp(z' - z) x(z', s) , \quad (1)$$

where  $\gamma(z, s)$  is the beam energy at position  $s$  in units of  $mc^2$ ;  $\rho$  is the line density of the particles in the bunch normalized to the total number of particles in the bunch  $N$ ;  $eW_\perp x$  is the transverse field produced by a point charge displaced from the axis by  $x$  at a distance  $z' - z$  behind that point charge;  $\lambda(z, s)$  is the betatron wavelength; and  $r_0 = e^2/mc^2$  is the classical radius of the electron. In writing this equation of motion we have assumed that the betatron focusing is provided by a smooth function rather than from a series of discrete quadrupole magnets.

We assume that the beam energy increases linearly with  $s$  as a result of acceleration, such that  $\gamma(s) = \gamma_0(1 + Gs)$ , where  $\gamma_0$  is the injection energy and  $G$  is the accelerating gradient. If we assume that the distance to double the energy is long compared to the betatron wavelength (equivalently,  $k \gg G$ ), then Eq. (1) can be written:

$$\frac{d^2}{ds^2} x(z, s) + k^2(z, s) x(z, s) = \frac{r_0}{\gamma(z, s)} \int_z^\infty dz' \rho(z') W_\perp(z' - z) x(z', s) , \quad (2)$$

where we have defined  $k(z, s) = 2\pi/\lambda(z, s)$ .

To find the conditions for auto-phasing we attempt to find an identical solution for all particles independent of longitudinal position within the bunch. Let us consider an expression of the form

$$x(z, s) = x_0 \cos(k_0 s + \phi_0) , \quad (3)$$

where  $\phi_0$  is an arbitrary initial phase, and derive the condition that needs to be satisfied in order for this expression to be a solution to Eq. (2). Inserting Eq. (3) into

Eq. (2) and noting that Eq. (3) is independent of  $z$ , and hence that it can come out of the integral, we find

$$k^2(z, s) = k_0^2 + \frac{r_0}{\gamma(z, s)} \int_z^\infty dz' \rho(z') W_\perp(z' - z) . \quad (4)$$

In order to gain some insight into the purpose of the previous mathematical manipulations, we first discuss the meaning of Eq. (4) and then we come to the solution of the equation of motion, Eq. (3). A particle at position  $z$  within the bunch, subjected to wakefield forces from all the other particles ahead in the bunch, will experience a frequency shift given by the second term on the right-hand side of Eq. (4). The first term on the right-hand side is the square of the frequency with which all particles are required (by the form of the solution) to oscillate. For this condition to be possible, the external focusing forces must be such that when they act *alone* on the particle, its betatron oscillation frequency is given by  $k(z, s)$ . Hence, by carefully balancing the two frequencies—one coming from the chromatic effects, the other from the transverse wakefield effects—all particles in the bunch will oscillate with the same amplitude, phase, and frequency, as Eq. (3) suggests. It is important to note that the auto-phasing condition, Eq. (4), is independent of the transverse offset  $x_0$  of the bunch. This condition is to be satisfied at all linac positions  $s$ .

To further realize the significance of this result, suppose that a dipole-like error perturbs the trajectory of a bunch along the linac, giving rise to a betatron oscillation. Since the auto-phasing condition is independent of the transverse displacement, it still holds true in the presence of betatron oscillations of arbitrary amplitude, and hence in the presence of any type of errors causing betatron oscillations in the machine! Dipole-like errors may come from injection errors in position and angle, from quadrupole displacements, RF kicks, or dipole strength changes. In the presence of any of these errors, the bunch will remain “compact,” maintaining the beam emittance constant. Further, this technique is expected to work successfully for any charge density, as long as Eq. (4) is satisfied for each point in the linac, thus ensuring the emittance preservation throughout the whole machine! [It should be pointed out that chromatic effects can still occur when beam steering is done on a scale that is short when compared to  $\lambda(s)$ .]

We conclude this section by pointing out the differences between BNS damping, as routinely used in the SLC linac for transverse wakefield control,<sup>5</sup> and auto-phasing. As explained earlier, the technique of auto-phasing provides compensation of the forces acting on the bunch independently of any dipole-like kicks along the trajectory of the bunch. On the other hand, BNS, as presently used in the SLC, best handles injection launch errors and (much less so) errors originating midway along the machine. Another important difference is that present BNS damping minimizes the beam emittance *only* at the end of the linac; at all other points along the linac, the projected phase-space volume occupied by the beam can assume larger values.

With the use of auto-phasing, however, the beam emittance stays near a minimum value everywhere along the linac. This is because the forces are compensated for locally, thus not allowing the emittance to grow. The net offset of the beam at the linac end is removed by position feedback. Schematic examples of the effects of these different techniques on the beam emittance along the linac are shown in Fig. 1. The curve corresponding to auto-phasing represents the theoretically expected goal of the method: namely, the fractional emittance enlargement stays close to one throughout the whole linac.

Next we demonstrate how the lattice parameters can be adjusted so that the external energy-dependent forces compensate the internal wakefield forces, and the condition for auto-phasing is satisfied.

#### 4. LATTICE ADJUSTMENT: $k_E$

Let us define  $k_W(z)$  as the right-hand side of the auto-phasing condition, Eq. (4),

$$k_W(z) = k_0^2 + \frac{r_0}{\gamma(z)} \int_z^\infty dz' \rho(z') W_\perp(z' - z) \quad (5)$$

The subscript  $W$  serves as a reminder that this expression depends on the wakefields and on the internal parameters of the bunch. The goal now is to adjust the quadrupole lattice and klystron phasing so that the energy-dependent forces cancel the transverse wakefield forces at all points in the linac. Equivalently, we need to determine an energy-dependent function of  $z$ ,  $k_E(z)$ , such that

$$k_W(z) = k_E(z) \quad (6)$$

In Fig. 2 we give a pictorial representation of Eq. (6). Figure 2(a) is a plot of the bunch density along the bunch. The Gaussian bunch length in this example is 1.75 mm and we assumed  $3.5 \times 10^{10}$  particles per bunch. Figure 2(b) displays the integrated transverse wakefield as a function of the longitudinal position  $z$ . By adding the frequency of the bunch head  $k_0$  to the integral according to Eq. (5), we obtain Fig. 2(c) which is a plot of  $k_W$  as a function of  $z$ . Figure 2(d), on the other hand, shows the beam energy along the bunch. Longitudinal wakefields have been taken into account and the klystron phase has been chosen to be  $8^\circ$  in this particular example. Finally, Fig. 2(e) is a plot of the betatron frequency along the bunch as determined from lattice considerations and the bunch energy. The goal is to match the shape of Fig. 2(c) to the shape of Fig. 2(e) by varying the bunch length and the klystron phases.

From the definition of the chromaticity of a lattice  $\xi$ :

$$\frac{\delta\nu}{\nu} = \xi \frac{\delta E}{E} \quad (7)$$

$k_E$  is given by

$$k_E(z) = k_0 \left[ \frac{E_0 + \xi(E(z) - E_0)}{E_0} \right] \quad (8)$$

where  $E_0$  is the energy of the head of the bunch. As expected, a less energetic particle will oscillate with higher betatron frequency. The energy  $E(z)$  corresponding to the betatron wave number  $k_E(z)$  is given by

$$E(z) = E_{inj} + \sum_{i=1}^n \left[ \Delta E_i \cos(\phi_i + \phi(z)) + \Delta s_i \int_z^\infty W_{\parallel}(z' - z) \rho(z') dz' \right] \quad (9)$$

where  $E_{inj}$  is the injection energy;  $\phi_i$  are the klystron phases (which are free parameters);  $\phi(z) = 2\pi z/\lambda_{RF}$ , where  $\lambda_{RF}$  is the RF wavelength;  $\Delta E_i$  is the maximum energy gain in the distance  $\Delta s_i$ ; and the last term on the right-hand side of Eq. (9) is the longitudinal wakefield contribution to the particle energy.

Thus the goal of lattice parameter adjustment is to determine the values of the bunch length and the klystron phases so that  $k_E = k_W$  at every point along the bunch and the linac. In the following section we use the SLC linac as an example to demonstrate how this careful matching can be done in a realistic situation.

#### 5. AUTO-PHASING APPLIED TO THE SLC

The applicability of auto-phasing to the SLC linac was studied with the goal of potentially improving the luminosity. A computer program was written to match the lattice and wakefield-determined spatial frequencies  $k_E(z)$  and  $k_W(z)$  over the length of a bunch at every longitudinal position along the linac. In parallel, a proposal to experimentally study this effect on the SLC has been made.<sup>6</sup>

Computation inputs were made as realistic as possible. The injection energy was 1.15 GeV. The acceleration was 1.8 GeV per 100 m. The linac was broken into eight sections of length 100 m, 200 m, 400 m, 400 m, 400 m, 400 m, 500 m, and 500 m, respectively, for a total length of 2900 m. The phases of all klystrons within a section were set to the same value, but allowed to vary as a group. The nominal betatron wavelengths were set to 25 m in the first section, 50 m in the second, and 100 m thereafter. The lattice had a phase advance of  $90^\circ$  per cell with a chromaticity value of  $-1.27$ . The betatron focusing was assumed to be provided by a smooth function. A study of the effects of discrete quadrupoles on auto-phasing is underway. The transverse and longitudinal wakefields were those calculated for the SLAC linac.<sup>7</sup>

The match conditions were calculated by numerical integration over the bunch divided into 61 longitudinal slices of length 0.25 mm. The number of particles in each slice was determined using the bunch (Gaussian) width and the total beam charge. The transverse and longitudinal wakefields and the energy profile along the bunch were calculated from this density profile, the accelerating structure, and the klystron

phases. The nominal head of the bunch was taken to be the slice  $2\sigma_z$  in front of the core.

The match of  $k_E(z)$  and  $k_W(z)$  at the end of a given linac section was accomplished by determining the best phase for that section, given the input bunch length and charge. Once the optimum was obtained, the program advanced to the next section. The upstream optima were used in downstream calculations. Since  $k_E(z)$  and  $k_W(z)$  in principle cannot match over a long distance, a weight function  $D$  was used for minimization,

$$D = \sum_{i=1}^{61} \rho(z_i) (k_E(z_i) - k_W(z_i))^2 \quad (10)$$

This function proved to be satisfactory and efficient.

The auto-phasing match was studied for 6 SLC linac conditions, assuming  $3.5 \times 10^{10}$  particles per bunch. Non-BNS and presently used BNS solutions are included for comparison. The functions shown in the following plots resulting from the calculations are for  $k_E(z)$ ,  $k_W(z)$ , and  $\rho(z)$  at four locations in the linac. However, all eight sections were calculated or optimized. The locations plotted were chosen to be separated by roughly factors of three in beam energy. Only in Cases 1, 2, and 6 was the energy spectrum minimized at full energy.

- Case 1. The results from SLC linac conditions without optimization or BNS damping, but with phases set to minimize the final energy spectrum are shown in Fig. 3. The auto-phasing match is not good, as shown by the separation of  $k_E$  and  $k_W$  in the region of the bunch core.
- Case 2. The second result represents the presently used BNS damping conditions and is shown in Fig. 4. Again, the match is not very different from the non-BNS case. The final energy spectrum is about 0.3%.
- Case 3. Here the bunch length is set to 1 mm and the program is allowed to minimize the separation of  $k_E$  and  $k_W$  (see Fig. 5). The match is now much better, although the internal frequencies of the two curves do not quite match. The final energy spectrum has risen to 0.76%.
- Case 4. The bunch length was increased to 1.75 mm and the phases then were optimized. The results are shown in Fig. 6. A very good match is obtained over the entire bunch; the internal frequencies of the curves match very well. The final energy spectrum is 1.4%.
- Case 5. This case uses a bunch length of 2.5 mm (see Fig. 7) but cannot be optimized as well as the 1.75 mm case. The internal frequencies of the two curves do not match again. The energy spectrum is 2.3%.
- Case 6. The energy spectrum at the end of the linac needed for the final focus is below 0.5%. In this last case, a 1.75 mm optimized solution (shown in Fig. 8) has the phase of the last 500 m of the linac set to make a small energy spectrum. A phase of  $+47^\circ$  is required in that region, which may be operationally

cumbersome. The auto-phasing condition is matched in all but the last region. Extending this phase adjustment over more sections may help the energy spectrum and phase offset, but will affect the auto-phasing match. The tradeoffs will be studied; however, there appears sufficient energy in the SLC RF system to permit auto-phasing at  $3.5 \times 10^{10}$  particles per bunch. This scenario is worth experimental investigation.

## 6. CONCLUSIONS

In this paper we have studied the requirements of auto-phasing. By carefully matching the internal bunch parameters with external forces, mutual compensation of transverse and chromatic effects for intense electron bunches can be achieved. With this compensation it is expected that the alignment and launch tolerances can be significantly relaxed.

We started from the equation of motion of a particle in the presence of transverse wakefields and derived the condition for auto-phasing. We then discussed the physical meaning of the result and concluded that its significance lies in the fact that the bunch will remain coherent in its motion independently of any dipole-like perturbations to its trajectory, and hence the emittance ideally will remain unchanged.

These results were then applied to the SLC linac. In our numerical computations we used the transverse and longitudinal wakefields calculated for the SLAC linac, but assumed smooth focusing. We determined the appropriate klystron phases and bunch lengths for auto-phasing to hold in several positions in the linac. These initial studies indicate that auto-phasing is possible for the SLC, and that more studies and possibly beam experiments should be pursued. Additional studies of tolerances and applicability using FODO lattices are being made. The effects of non-Gaussian bunch shapes (e.g., those produced by the SLC bunch length compression system) will also be studied, and reported elsewhere.

## REFERENCES

1. J. T. Seeman, "Beam Dynamics Issues in Linear Colliders," *Proc. 1989 IEEE Part. Acc. Conf.*, Chicago, p. 1736; SLAC-PUB-4886 (1989).
2. V. Balakin, A. Novokhatsky, and V. Smirnov, "VLEPP: Transverse Beam Dynamics," *12th Int. Conf. on High Energy Acc.*; FNAL (1983), p. 119.
3. V. Balakin, *Proc. 1988 Workshop on Linear Colliders*, SLAC-Report-355 (1988), p. 55.
4. A. W. Chao, B. Richter, and C.-Y. Yao, "Beam Emittance Growth Caused by Transverse Deflecting Fields in a Linear Accelerator," *Nucl. Instrum. Methods* **178**, 1-8 (1980).
5. K. Banc, "Landau Damping in the SLAC Linac," *IEEE Trans. Nucl. Sci.* **NS-32**, 2398 (1985).
6. V. Balakin, V. Parkhomchuk, and V. Shiltsev, "The Experimental Examination of 'Autophasing for Transverse Oscillations' on the SLC at SLAC," Proposal from the Institute of Nuclear Physics, Novosibirsk, August 1989.
7. K. Bane and P. Wilson, "Longitudinal and Transverse Wake Potentials in SLAC," *Proc. 11th Int. Conf. on High Energy Acc.*, CERN (Birkhäuser Verlag, Basel, 1980), p. 592.

## FIGURE CAPTIONS

1. Emittance enlargement (effective) for the cases of no damping, present BNS damping, and auto-phasing. In the case of auto-phasing, the curve represents the theoretically expected goal of the method.
2. Schematic representation of the mutual compensation of wakefield and chromatic effects of a bunch. This example is taken at the 100 m position in the linac.
3. Case 1. Klystron phases  $\phi_i = 8^\circ$  for all eight sections; bunch length  $\sigma_z = 1$  mm; and final energy spread  $\sigma_E/E = 0.29\%$ .
4. Case 2. Klystron phases  $\phi_i = -25^\circ, -25^\circ, -25^\circ, 18^\circ, 18^\circ, 18^\circ, 18^\circ, \text{ and } 18^\circ$ ; bunch length  $\sigma_z = 1$  mm; and final energy spread  $\sigma_E/E = 0.30\%$ .
5. Case 3. Klystron phases  $\phi_i = -3^\circ, -7^\circ, -20^\circ, 5^\circ, 5^\circ, 6^\circ, 6^\circ, \text{ and } 6^\circ$ ; bunch length  $\sigma_z = 1$  mm; and final energy spread  $\sigma_E/E = 0.76\%$ .
6. Case 4. Klystron phases  $\phi_i = -7^\circ, -10^\circ, -20^\circ, -1^\circ, -1^\circ, 0^\circ, 0^\circ, \text{ and } 0^\circ$ ; bunch length  $\sigma_z = 1.75$  mm; and final energy spread  $\sigma_E/E = 1.40\%$ .
7. Case 5. Klystron phases  $\phi_i = -8^\circ, -11^\circ, -19^\circ, -3^\circ, -3^\circ, -2^\circ, -2^\circ, \text{ and } -2^\circ$ ; bunch length  $\sigma_z = 2.50$  mm; and final energy spread  $\sigma_E/E = 2.30\%$ .
8. Case 6. Klystron phases  $\phi_i = -7^\circ, -10^\circ, -20^\circ, -1^\circ, -1^\circ, 0^\circ, 0^\circ, \text{ and } 47^\circ$ ; bunch length  $\sigma_z = 1.75$  mm; and final energy spread  $\sigma_E/E = 0.53\%$ .

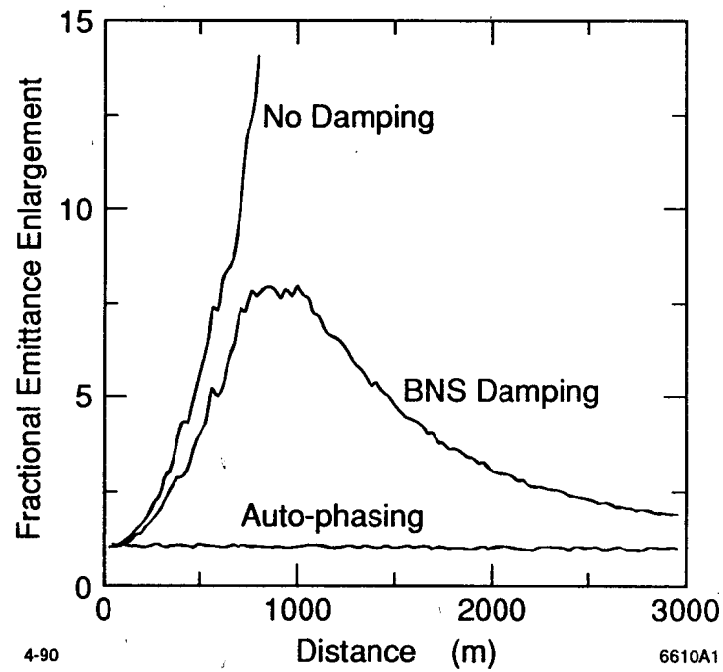


Fig. 1

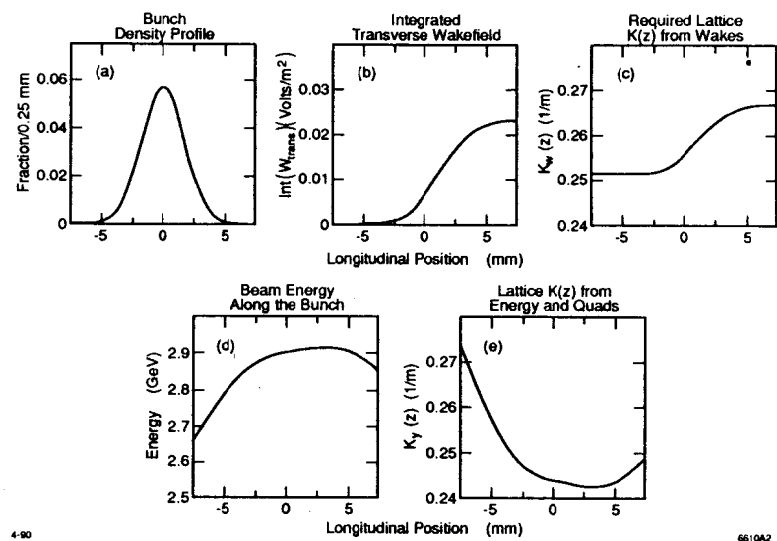


Fig. 2

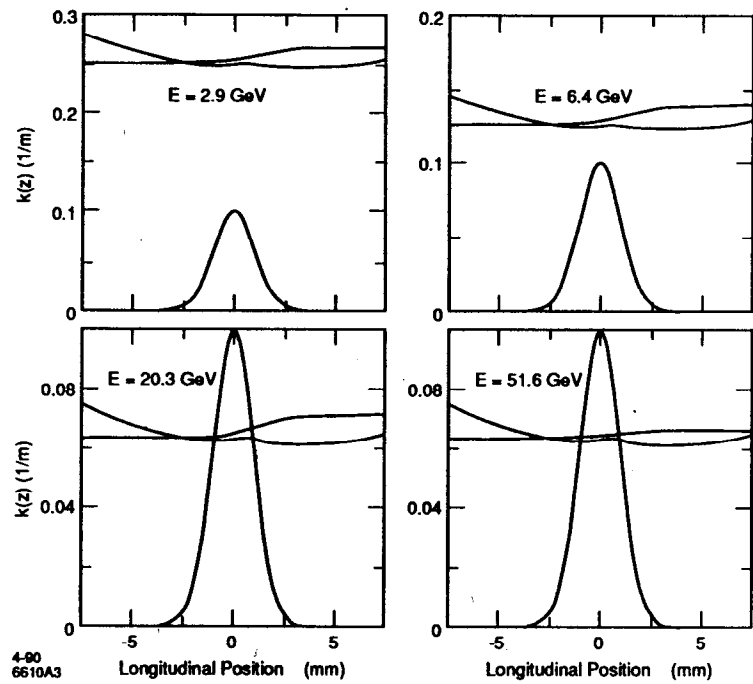


Fig. 3

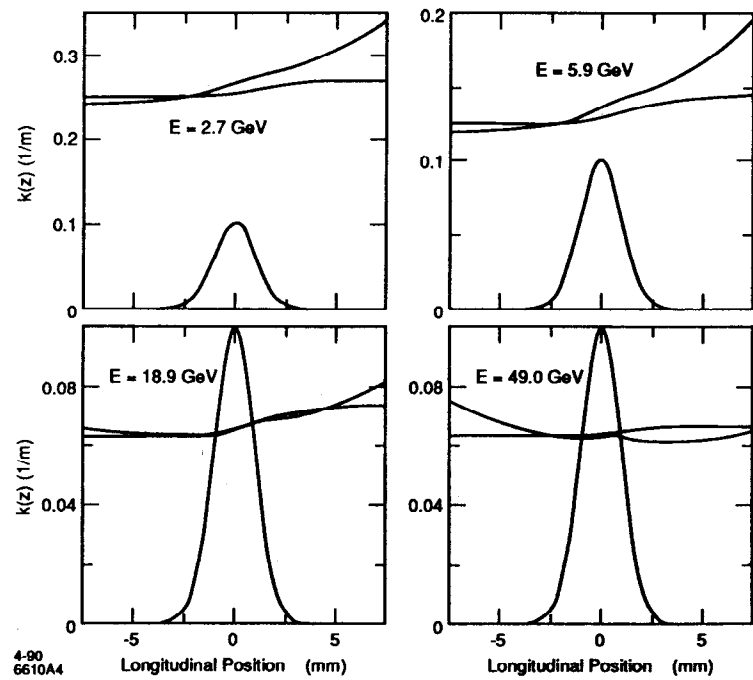


Fig. 4

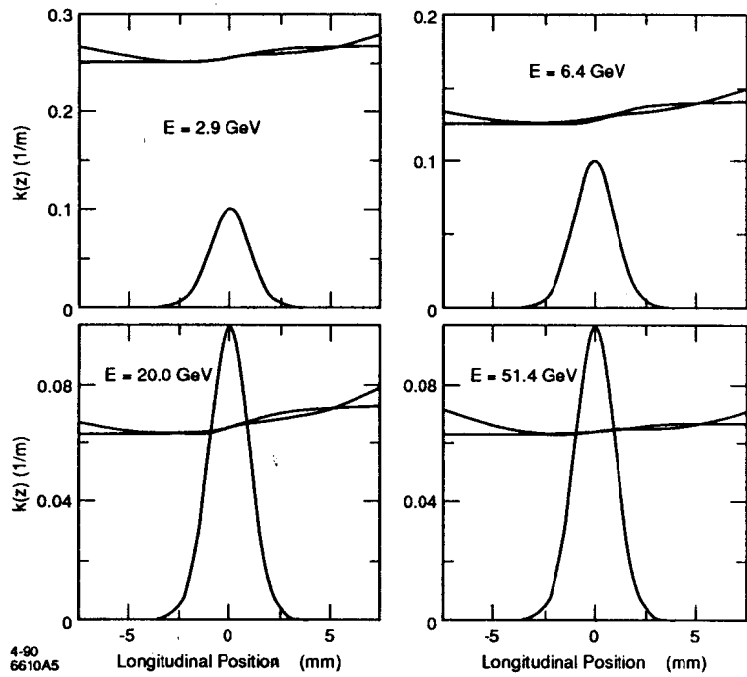


Fig. 5

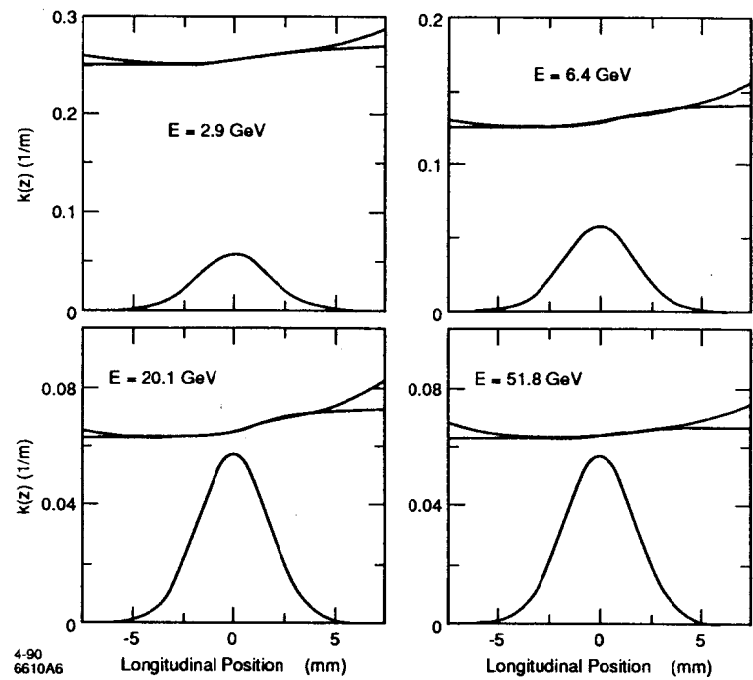


Fig. 6



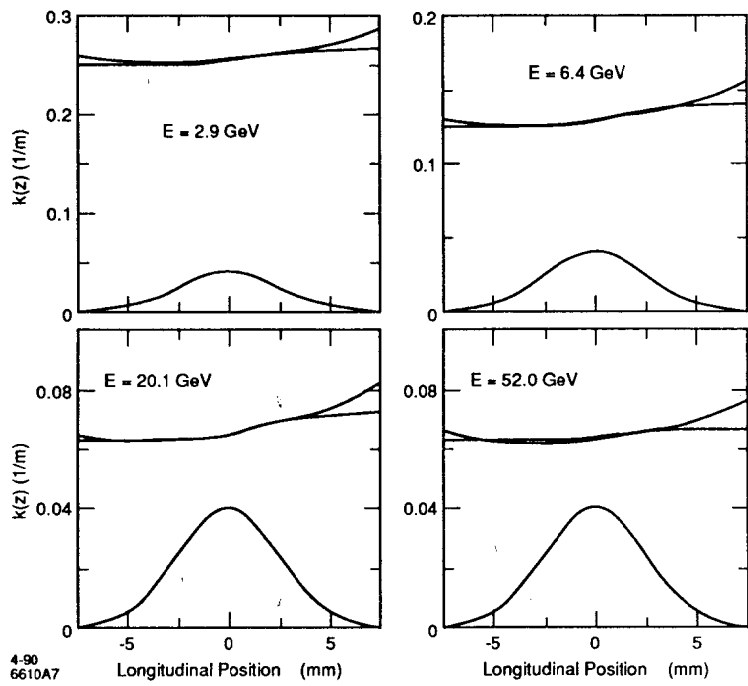


Fig. 7

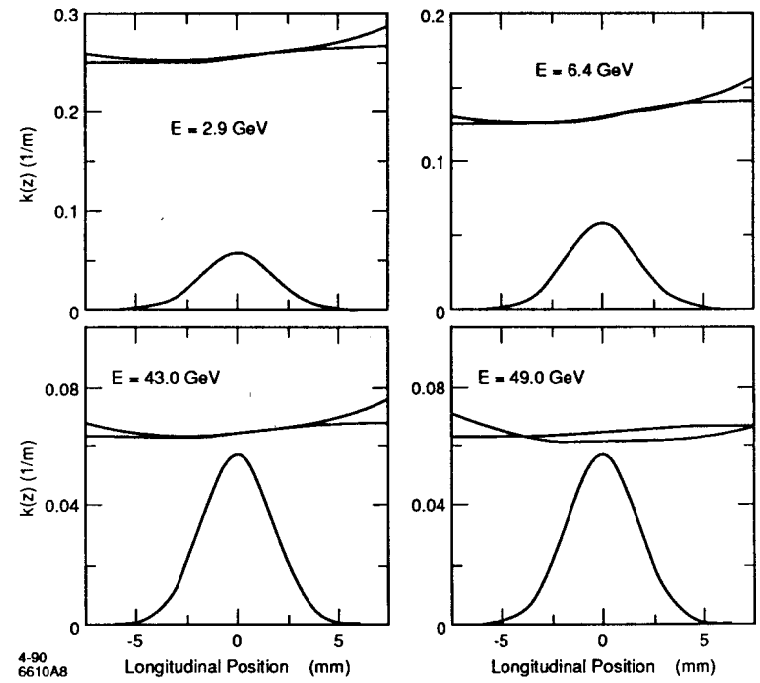


Fig 8